



Analyse fréquentielle des débits de crues avec des données historiques en prenant en compte les erreurs aléatoires et systématiques

Luc Neppel, Benjamin Renard, Michel Lang, Pierre Alain Ayrat, Denis Coeur, Eric Gaume, Nicolas Jacob, Olivier Payrastre, Karine Pobanz, Freddy Vinet

► To cite this version:

Luc Neppel, Benjamin Renard, Michel Lang, Pierre Alain Ayrat, Denis Coeur, et al.. Analyse fréquentielle des débits de crues avec des données historiques en prenant en compte les erreurs aléatoires et systématiques. Hydrological Sciences Journal, 2010, 55 (2), pp 192-208. 10.1080/02626660903546092 . hal-00509088

HAL Id: hal-00509088

<https://hal.science/hal-00509088>

Submitted on 15 May 2020

HAL is a multi-disciplinary open access archive for the deposit and dissemination of scientific research documents, whether they are published or not. The documents may come from teaching and research institutions in France or abroad, or from public or private research centers.

L'archive ouverte pluridisciplinaire **HAL**, est destinée au dépôt et à la diffusion de documents scientifiques de niveau recherche, publiés ou non, émanant des établissements d'enseignement et de recherche français ou étrangers, des laboratoires publics ou privés.

Flood frequency analysis using historical data: accounting for random and systematic errors

LUC NEPPEL¹, BENJAMIN RENARD², MICHEL LANG², PIERRE-ALAIN AYRAL³,
DENIS COEUR⁴, ERIC GAUME⁵, NICOLAS JACOB⁶, OLIVIER PAYRASTRE⁷, KARINE
POBANZ², FREDDY VINET⁸.

1 UMR HydroSciences Montpellier – Université Montpellier II – place Eugène Bataillon – CC MSE – 34090
Montpellier Cedex 5, France. – neppel@msem.univ-montp2.fr

2 Cemagref Lyon – Hydrology Hydraulics – 3 bis quai Chauveau – CP 220 – 69336 Lyon cedex 09, France.

3 Ecole des Mines d'Alès, LGEL, 6 av de Clavières, 30 100 Alès, France

4 ACTHYS Diffusion, 253, chemin de Plate-Rousset, 38 330 Biviers, France

5 LCPC, Route de Bouaye, BP 4129, 44341 Bouguenais cedex, France

6 Université de Lyon II - UMR 5600 – 5 avenue Pierre Mendès –France 69676 Bron cedex, France

7 SPC Grand Delta du Rhone, DDE du Gard, 89, rue Weber, 30907 Nimes cedex, France

8 UMR Gester,, Université Montpellier III, Route de Mende, 34199 Montpellier Cedex 5, France

Abstract :

This paper presents a flood frequency analysis (FFA) based on a set of systematic data and a set of historical floods, applied to several Mediterranean catchments. After identification and collection of data on historical floods, several hydraulic models were constructed to account for geomorphological changes. Recent and historical rating curves were constructed and applied to reconstruct flood discharge series along with their uncertainty. This uncertainty stems from two types of errors: (a) random errors related to the water level readings; (b) systematic errors related to over- or underestimation of the rating curve. A Bayesian frequency analysis is performed to take both sources of uncertainty into account. It is shown that: (a) the uncertainty affecting discharges should be carefully evaluated and taken into account in the FFA, as it can increase the quantiles confidence interval; (b) the quantiles are

found consistent with the ones obtained with empirical methods, for two out of four of the catchments.

Keyword :

Historical flood, Bayesian flood frequency analysis, discharge errors, Mediterranean catchment

I. INTRODUCTION

The most widely used method for flood frequency analysis is to estimate the parameters of a probability distribution using a sample of observed flood events. As discharge time series are often short compared to the recurrence interval of the quantiles of interest, this method is highly sensitive to the sampled data. In France, for example, the longer uninterrupted discharge series provide 40 to 50 years of data, with only a couple of series longer than 80 years (Renard, 2006), whereas flood-risk areas are defined on the basis of a design event with a recurrence interval of at least 100 years. One way of reducing the resulting uncertainties is to extend the observation period by augmenting the systematic observations with historical flood events or paleofloods. A number of applications – for example, Llasat *et al.* (2005) in Catalonia; Naulet *et al.* (2005) on the Ardèche river (France); and Payrastre *et al.* (2005, 2006) on small watersheds in the Aude river system (France) – demonstrate the improvement offered by this method compared to methods using only the systematic observation period. Brazdil *et al.* (2006) provide a more detailed assessment of flood risk that takes account of historical flood events in Europe.

A first difficulty with this approach lies in the estimation of empirical flood frequencies from a sample made of both systematic and censored data. Indeed, historical discharge data are not exhaustive: only events exceeding a given threshold of perception (possibly varying over time) are reported. Hirsh and Stedinger (1987) and Naulet (2002) propose ways of computing empirical flood frequencies with a mixed systematic/censored sample. A second difficulty is to quantify the discharge of historical flood events, as this information is often subject to considerable uncertainty, which must be taken into consideration in estimating flood frequency. Moreover, such error is not limited to historical floods; it also affects more recent exceptional events for which only posterior estimates of discharge are available (Gaume *et al.*, 2004; Sheffer *et al.*, 2008). It can be considered that the data on historical flood events are marred by random errors related to readings of the staff gauge, and both historical and recent flood events are marred by systematic errors arising from over- or underestimation of the rating curve.

This paper presents a frequency analysis method that takes these two sources of error into account for floods in both the historical and systematic periods. The approach presented was developed under the INONDHIS-LR project (Neppel *et al.*, 2007), funded by the French Ministry of Ecology. The second section presents the study area and the data. The third section describes the frequency analysis models, with an application to a Mediterranean catchment. The results of the analysis are further discussed in the fourth section.

II. STUDY AREA AND DATA

1. Location of the study area

The INONDHIS-LR project studies ten Mediterranean catchments: two in the Hérault river system, four in the Aude and four in the Gard watershed. This paper considers the latter catchments, particularly the catchment of the Gardon d'Anduze river at Anduze, which has an area of 540 km², making it – along with the Gardon d'Alès (320 km²) – one of the main tributaries of the Gard river, which drains a total area of about 2000 km² into the Rhône river (Figure 1).

The two main tributaries of the Gardon d'Anduze are the Gardon de Saint-Jean (154 km²) and the Gardon de Mialet (219 km²). Their catchments are bounded on the north by the crests of the Cévennes range, which can exceed 1000 mNGF¹ in altitude, and their outlets lie at altitudes around 100 m. Given the steep gradients of the catchments and the torrential rainfall characteristic of the Mediterranean rim in autumn, these streams are the site of devastating floods (Ayrat, 2004; Marchandise, 2007).

The four catchments in the Gard system are instrumented by gauging stations belonging to the Grand Delta flood forecasting department (FFD), formerly the flood warning department (FWD), founded in 1892. The purpose of these measurements was not to compile a time series of discharge data for hydrological analysis, but to provide flood warning. Managers were therefore interested in the flood crest levels rather than in discharge *per se*, which explains the virtual absence of gaugings (there are only two low-flow gaugings at the Anduze station). The possibilities for gauging discharge during flood events are severely limited by the high flow velocity. Incidentally, this is why a majority of hydrometric stations in the Mediterranean region are not gauged beyond the 2-year flood (Lang *et al.*, 2006). The Grand Delta FFD allowed the authors of this paper to use the topographical surveys conducted in

¹ NGF = *nivellement général de la France*, the altitude reference system of France's National Geographical Institute (IGN).

2003 for all catchments in the Gard river system, with longitudinal profiles and latitudinal profiles from 40 to 300 metres apart.

2. Available historical data

The work of identifying historical information, collecting it from archives and subjecting it to critical analysis was conducted in conjunction with historians and geographers. The methods used are not described in this paper; for a description, see Cœur *et al.* (2002) or Naulet *et al.* (2005). The data relate either to flood crest levels or to the morphology of the Gardon.

For this sector, a total of 249 useable flood crest measurements were found, the oldest dating from 1741. When their positions were given with respect to a landmark still in existence, it became possible to place them in the NGF system. Some archives provided only censored information owing to the lack of precision of observations, e.g. “the water level is above the bridge parapet”. Figure 2 lists all the flood events found for the Gardon d’Anduze; the series is incomplete for the 1741-1891 period (high water mark, threshold level not exceeded, measurement recorded as an interval) and complete since 1892. The FFD archives contributed greatly: the entire series of daily water-level measurements were found for the four catchments studied, dating back to the founding of FWD in 1892. The past positions and zero levels of the staff gauges were reconstructed, partly from correspondence between FFD engineers and the observers assigned to each sector, and partly from breaks in the time series of low-water levels.

Historical information on the morphology of the Gardon stems from technical studies for hydraulic works and reports on major hydrometeorological events. The plans, consisting of

longitudinal profiles and a few latitudinal profiles, show the crest levels of known major flood events. The period from 1845-1850 to the present, was marked by a deepening of the streambeds, by more than three metres in some areas. This phenomenon, which has also been evidenced in a nearby area through analysis of lichens (Gob *et al.*, 2008), results from an incision in the gravelly alluvium and the gradual scouring out of this material once sedimentary build-up in the channels stopped in these catchments. As in most watercourses in the Rhône watershed, the process seems irreversible as from the 1950s. Figure 3 presents a 3 km stretch of the Gardon d'Anduze at Anduze. Comparing the oldest useable profile, dating from 1849, to that produced in the 2003 survey, it can be seen that the river bed has sunk by approximately 2 m on the downstream side of the Anduze bridge.

3. Example of reconstruction of flood discharges at Anduze

Estimates of flood discharge are based on hydraulic modelling of a reach about 2 km long. The river bed was fairly stable at the downstream end between the 1849 and 1985 profiles (Figure 3), then deepened by about 1.5 m between 1985 and 2003. We therefore use two models: a “recent” model based on the 2003 topographical surveys supplemented by Cemagref's 2006 surveys and applied to the period from 1985 onward; and a “historical” model obtained by raising the river bed floor by 1.50 m. Considering the consistency between 1849 and 1985 profiles, the latter is considered to be representative of the streambed topography for the historical period. The historical profiles collected did not allow to reconstruct the river's topographical past with sufficient precision to refine the hydraulic models further.

Discharge estimates are based on numerical solutions of Barré de Saint Venant's free surface runoff equations (Chow, 1960), in a one-dimensional simulation using the Manning-Strickler discharge formula. The software used was RUBARBE (Paquier and Khodashenas, 2002), which divides the river's geometry into a low flow channel and a floodplain. The software makes it possible to model a change from sub-critical flow to torrential flow.

The first step in hydraulic modelling is to calibrate the model, i.e. to determine the Manning coefficients. The calibration procedure is performed in two steps (main channel/floodplain), and is described in greater detail in Renouf *et al.* (2005) and Lang *et al.* (2006). For the main channel, calibration is performed using stream gaugings. A first Manning coefficient is estimated based on the (water level;discharge) observations. An uncertainty of +/-5 cm for water level and +/-10% for discharge is then considered. A second calibration procedure is performed using the values (water level minus 5 cm, discharge plus 10%) and (water level plus 5 cm, discharge minus 10%). This leads to an interval for the Manning coefficient in the main channel, which corresponds to an envelop curve of the rating curve (Figure 4). This approach is applied with two gaugings available at Anduze, corresponding to low discharges in the main channel. The corresponding Manning coefficient ranges from 1/30 to 1/20. In the floodplain, no measurements were available, so the Manning coefficient is restricted to the interval 1/20- 1/10, based on field observations and the configuration of the floodplain (see correspondence tables, Barnes, 1967).

The second step is to construct rating curves in the staff gauge cross-section. For each model (historical and recent), the primary relationship between discharge and water level is determined, then a range for this relationship is derived from the uncertainty bounds on the Manning coefficient, as explained on figure 4. Figure 5 presents the rating curves obtained.

One can notice on figure 5 that the upper limit of the rating curve described by the rating curve error model doesn't correspond to the previous one by hydraulic sensitivity analysis (i.e the envelop curve related to the sensitive analysis on Manning coefficient). The hydraulic analysis showed that if supercritical flow appears in the neighbourhood of the bridge for the three curves (respect. upper, central and lower) for respectively $Q = 4000$, 5000 and $6000 \text{ m}^3/\text{s}$, the position of the hydraulic jump is either just in front of the flood scale (upper curve) or upstream the flood scale (central and lower curves). The former case leads to an equivocal relationship between stage and discharge, but a large uncertainty remains on the exact location of the hydraulic jump. As such hypothetical upper limit yields values that are much too high in terms of specific discharge, it has been considered to be overestimated. The rating curve error model was therefore calibrated without hydraulic jump.

Once the rating curves have been constructed for both the recent and historical models, the sample of flood level measurements is used to construct the sample of discharge values. Figure 2 shows the series of reconstructed discharge values from 1741 to 2005. Discharges have been estimated using the central rating curves in figure 5 (the uncertainty related to a possible systematic rating curve error is therefore not represented in figure 2). It can be observed that this data series is made of several data types:

- Point-values (circles) correspond to water level data known with high precision. Discharges corresponding to such data are therefore solely affected by the uncertainty stemming from rating curve errors (not represented in figure 2).
- Intervals correspond to water level data known with limited precision. The information therefore consists of lower and upper bounds for the water level reached during the flood. This water level interval can be transformed into a discharge interval using the central rating curve.

- The perception threshold (horizontal line) corresponds to the water level ensuring the exhaustiveness of historical data collection. In other words, it can be ensured that water levels did not exceed the perception threshold during years with no available information in figure 2 (otherwise, such event would have been recorded in the historical archives).

The five highest flood levels recorded at Anduze are those of 1958 (7.6 m; 4575 m³/s), 1861 which ranked between 7m (4100 m³/s) and 8.2 m (5600 m³/s), 1890 (7.1 m; 4260 m³/s), 1846 and 1847 (7.0 m; 4135 m³/s). For the flood event of 9 September 2002, the gauge reading was initially recorded as 7.60 m in the FWD survey, but a review led to it being adjusted to and ultimately validated at 5.60 m with hydraulic modelling, as the initial reading proved inconsistent with the high-water marks available in the vicinity. The interpretation adopted jointly with the FFD is that the reading was taken upstream of the Anduze road bridge, whereas the gauge is downstream. Given the very rough profile of the channel, the hydraulic model yields an estimate of 3500 m³/s with a very large error interval [2590 ; 5870 m³/s]. It should be noted that the value of 6180 m³/s that would have been obtained at Anduze (540 km²) at a flood crest of 7.60 m would also have been inconsistent from a hydrological standpoint when compared with the discharge estimate made by the FFD further downstream at Russans (1515 km²), which gave a range of 6000-6800 m³/s. The discharge interval used, [2590, 5870 m³/s], agrees with other estimates performed by DDE (2003) and the engineering firm ISL (2005), which range from 3000 and 3400 m³/s.

The flood of 9 September 2002 merits more detailed analysis because this event caused 23 deaths and an estimated €1.2 billion in damage (Huet *et al.*, 2003). In the upstream part of the Gardon d'Anduze catchment, this flood is not listed as a major event, while that of 1958

remains the biggest since 1741. This is consistent with the rainfall pattern that caused the 2002 flood, which was characterised by very high accumulations on the intermediate part of the catchment (Delrieu *et al.*, 2004), in contrast to the event of 1958, when the greatest cumulative rainfall was located in the foothills of the Cévennes range, upstream from Anduze (Jacquet, 1959). On the downstream part of the catchment, the flood is noteworthy for its geographical scope and an epicentre of over 600 mm at Lédignan (Neppel *et al.*, 2003). However, a paleohydrological analysis by Sheffer *et al.* (2008) in the canyons of the Gardon shows that the 2002 flood level has been exceeded at least five times over the last 500 years, based on sediment traces and dating of organic and mineral particles.

III. FREQUENCY ANALYSIS OF FLOOD DATA

The aim is to estimate flood quantiles from the samples collected for the recent and historical periods. This estimate needs to take account of the fact that the data are incomplete and that the discharge values are estimated using a hydraulic model and subject to considerable uncertainty.

The estimation of flood quantiles can be based on data extracted from two distinct sampling approaches. The peak-over-threshold (POT) approach uses flood peaks exceeding a predefined threshold. Since the exhaustiveness of data from the historical period is related to a perception threshold, it seems natural to use a POT approach, with a first exceedance threshold equal to the perception threshold during the historical period, and a second, lower, exceedance threshold during the systematic period. An example of POT-analysis of historical data can be found in the paper by Parent and Bernier (2003). Alternatively, historical data can also be included in the analysis of annual maxima (AM, see e.g. Naulet *et al.*, 2006). The

perception threshold is considered as a censoring threshold in this case. In this study, we opted for the AM approach.

The pros and cons of each approach for analyzing historical data are still unclear. An obvious drawback of the AM approach would be the loss of data if two (or more) floods happened to exceed the perception threshold within the same year. However, this is unlikely to occur with high perception thresholds. In particular, this did not occur in the dataset studied in this paper. A formal evaluation of the relative merits of the AM and POT approaches for analysing historical data would be of great interest; however, it is considered to lie beyond the scope of the present paper and is left for future work.

Let X_t be the random variable representing the “true” annual maximum discharge at the gauging station for year t ($t = 1, \dots, T$). Extreme value theory suggests using a generalized extreme value (GEV) distribution to model such data (e.g., Embrecht *et al.*, 1997). The probability density function f (pdf) and the cumulative density function F (cdf) of a $GEV(\mu, \lambda, \xi)$, where μ , λ and ξ are respectively the location, scale and shape parameters, are given by:

$$\begin{aligned} f(x | \mu, \lambda, \xi) &= (1/\lambda) [1 - \xi(x - \mu)/\lambda]^{-\frac{1}{\xi}-1} \exp\left\{-[1 - \xi(x - \mu)/\lambda]^{1/\xi}\right\} \\ F(x | \mu, \lambda, \xi) &= \exp\left\{-[1 - \xi(x - \mu)/\lambda]^{1/\xi}\right\} \\ \lambda &> 0; \xi \neq 0; 1 - \xi(x - \mu)/\lambda > 0 \end{aligned} \quad (1)$$

The case $\xi = 0$ corresponds to the Gumbel distribution, and is equal to the limit of equation (1) when $\xi \rightarrow 0$:

$$f(x|\mu, \lambda) = (1/\lambda) \exp\left\{-\frac{(x-\mu)}{\lambda} - \exp\left(-\frac{(x-\mu)}{\lambda}\right)\right\} \quad (2)$$

$$F(x|\mu, \lambda) = \exp\left\{-\exp\left(-\frac{(x-\mu)}{\lambda}\right)\right\}$$

$$\lambda > 0$$

269

270 The main task of frequency analysis is to estimate the parameter vector $\theta = (\mu, \lambda, \xi)$. A
271 Bayesian approach is used in this paper (e.g., Gelman et al., 1995). Standard frequency
272 analyses usually neglect the possible errors corrupting observed data. In this case, the
273 posterior distribution $p(\theta|X)$ is simply obtained by combining prior information on the
274 distribution of the parameters $p(\theta)$ and the likelihood of the observations vector $X=(X_t)_{t=1, \dots, n}$,
275 written as $p(X|\theta)$:

276

$$p(\theta|X) = \frac{p(X|\theta)p(\theta)}{\int p(X|\theta)p(\theta)d\theta} \propto p(X|\theta)p(\theta) \quad (3)$$

277 where the symbol ‘ \propto ’ denotes proportionality.

278

279 1. Error model

280 Unfortunately, the assumption that observed runoff data are error-free is untenable in most
281 applications involving historical data. An error model linking the “true” runoff X_t (which is
282 unknown, but whose distribution is wanted) with the “observed” runoff \tilde{X}_t (derived from a
283 hydraulic model) is needed. Further notation needs to be defined for this purpose.

284 Let H_t be the “true” water level reached during the highest flood of year t , and \tilde{H}_t the
285 corresponding observed level. When the historical information collected is deemed accurate
286 enough, or for data in the systematic measurement period, the error affecting observed water
287 level may be neglected, leading to the assumption $H_t = \tilde{H}_t$. However, incomplete information

may lead to relax this assumption, by simply assuming the true level is contained in an interval. This can be formalized as follows:

$$H_t = \tilde{H}_t + \delta_t, \delta_t \in [-l_t; l_t] \quad (4)$$

Using the above convention, the observed level \tilde{H}_t is the centre of the interval of length $2l_t$. Importantly, it will be assumed that the errors δ_t are independent from year to year. The rationale behind this assumption is that such errors are due to incompleteness or inconsistency of the historical information. The error made at year t should therefore not impact the error at year $t+1$, since it only depends on the availability and consistency of historical information. Runoff data are then derived by applying the rating curve obtained from the hydraulic model to the observed levels. Since several rating curves may be used, let $\hat{\psi}_k(h)$ denote the k th rating curve ($k = 1, \dots, N_c$). $\hat{\psi}_k(h)$ is an approximation of the “true” rating curve $\psi(h)$ linking the true runoff with the true water level. The following error model will be used to describe the error made during this approximation:

$$\psi(h) = \gamma_k \hat{\psi}_k(h) \quad (5)$$

This multiplicative error model is justified by the common observation that absolute rating curve errors (differences between true and estimated discharges) increase with the discharge value (e.g., Thyer et al., 2009; Reitan and Petersen-Overleir, 2009). Contrarily to water level errors, the rating curve error is systematic, i.e. all runoff data included in the period of validity of the k th rating curve are affected by the same multiplicative error γ_k . This error model is a particular case of the rating curve error model proposed by Kuczera (1996). Combining equations (4) and (5) allows deriving the relationship between true and observed runoff as follows:

$$\begin{aligned}
 X_t &= \psi(H_t) \\
 &= \gamma_k \hat{\psi}_k(H_t) \\
 &= \gamma_k \hat{\psi}_k(\tilde{H}_t + \delta_t) \\
 &= \gamma_k [\hat{\psi}_k(\tilde{H}_t) + \hat{\psi}_k(\tilde{H}_t + \delta_t) - \hat{\psi}_k(\tilde{H}_t)] \\
 &= \gamma_k [\tilde{X}_t^{(k)} + \hat{\psi}_k(\tilde{H}_t + \delta_t) - \hat{\psi}_k(\tilde{H}_t)] \\
 &= \gamma_k [\tilde{X}_t^{(k)} + \varepsilon_t], \\
 &\text{with } \varepsilon_t = \hat{\psi}_k(\tilde{H}_t + \delta_t) - \hat{\psi}_k(\tilde{H}_t)
 \end{aligned} \tag{6}$$

The superscript (k) has been introduced to recall the rating curve used to derive the observed runoff $\tilde{X}_t^{(k)}$. Since the additive water level error δ_t is included in the interval $[-l_t; l_t]$, the resulting additive runoff error ε_t is included in the interval $[\hat{\psi}_k(\tilde{H}_t - l_t) - \hat{\psi}_k(\tilde{H}_t); \hat{\psi}_k(\tilde{H}_t + l_t) - \hat{\psi}_k(\tilde{H}_t)] = [a_t; b_t]$.

The error model in equation (6) shows that observed runoff is affected by two different types of errors: a multiplicative systematic error stemming from the estimated rating curve, and independent event-specific errors stemming from the imperfect knowledge of the water level reached during historical floods.

2. Parameter estimation

In order to perform the Bayesian estimation of the GEV parameters, the likelihood of the observations $\tilde{X}_t^{(k)}$ needs to be derived. In a first step, inverting equation (6) gives the following relationship:

$$\tilde{X}_t^{(k)} = X_t / \gamma_k - \varepsilon_t \tag{7}$$

It is then possible to demonstrate that $p(\tilde{X}_t^{(k)} | \mu, \lambda, \xi, \gamma_k, \varepsilon_t)$, the distribution of an observation $\tilde{X}_t^{(k)}$, conditionally on errors γ_k and ε_t , is a $GEV(\mu / \gamma_k - \varepsilon_t, \lambda / \gamma_k, \xi)$ (see appendix 1).

The explicit treatment of errors leads to the introduction of additional unknown terms in the inference, namely vectors $\gamma=(\gamma_1,\dots,\gamma_{Nc})$ and $\varepsilon=(\varepsilon_1,\dots,\varepsilon_T)$. The length of vector γ is equal to the number of rating curves Nc used to reconstruct past discharges, which is likely to remain relatively small. However, the length of vector ε can theoretically be equal to the total number of years included in the analysis T . In practice, some components of ε can be fixed to zero, corresponding to flood events whose water levels are assumed to be known without any error (circles in Figure 2).

There are two options for treating these additional unknown terms: they can be included in the list of parameters to be estimated, or alternatively, they can be integrated out from the conditional distribution $p(\tilde{X}_t^{(k)} | \mu, \lambda, \xi, \gamma_k, \varepsilon_t)$ prior to the inference (e.g., Kuczera, 1992). In this paper, a mixed approach is adopted: parameter vector γ is included in the inference, but ε is integrated out as follows:

$$p(\tilde{X}_t^{(k)} | \mu, \lambda, \xi, \gamma_k) = \int p(\tilde{X}_t^{(k)} | \mu, \lambda, \xi, \gamma_k, \varepsilon_t) p(\varepsilon_t) d\varepsilon_t \quad (8)$$

Applying equation (8) requires defining a prior probability distribution for the error term ε_t . Since ε_t is assumed to be included in the interval $[a_t; b_t]$, a natural choice is to use the uniform distribution on this interval. This choice is particularly interesting because it allows performing the integration in equation (8) analytically (see appendix 2). Under this assumption, the distribution of an observation $\tilde{X}_t^{(k)}$, conditionally on errors γ_k only, is given by:

$$p(\tilde{X}_t^{(k)} | \mu, \lambda, \xi, \gamma_k) = \frac{1}{b_t - a_t} \left[F(\tilde{x}_t^{(k)} + b_t | \mu / \gamma_k, \lambda / \gamma_k, \xi) - F(\tilde{x}_t^{(k)} + a_t | \mu / \gamma_k, \lambda / \gamma_k, \xi) \right] \quad (9)$$

Note that in the particular case where ε_t is forced to zero (no water-level-related error), the conditional distribution $p(\tilde{X}_t^{(k)} | \mu, \lambda, \xi, \gamma_k)$ is simply given by:

$$p(\tilde{X}_t^{(k)} | \mu, \lambda, \xi, \gamma_k) = f(\tilde{x}_t^{(k)} | \mu / \gamma_k, \lambda / \gamma_k, \xi) \quad (10)$$

which appears to be the limit of the right hand side of equation (9) when $a_t \rightarrow b_t$.

Equations (9) and (10) can then be used to derive the likelihood function of the whole set of observations \mathbf{X} . For a given rating curve (k), let S_k be the set of years included in the period of validity of the rating curve for which an observation is available (either with point or interval water level data, corresponding to circles and intervals in figure 2). Let us further assume that n_k years correspond to censored data, i.e. the only available information is that the annual maximum flood did not exceed the perception threshold u_k . Lastly, it is assumed that annual maxima are independent and identically distributed. Under these assumptions, following Reis and Stedinger (2005), the likelihood function is proportional to:

$$p(\mathbf{X} | \mu, \lambda, \xi, \gamma) \propto \prod_{k=1, Nc} \left[\prod_{t \in S_k} \{ p(\tilde{X}_t^{(k)} | \mu, \lambda, \xi, \gamma_k) \} \right] [F(u_k | \mu / \gamma_k, \lambda / \gamma_k, \xi)]^{n_k} \quad (11)$$

In equation (11), the term $F(u_k | \mu / \gamma_k, \lambda / \gamma_k, \xi)$ is the cdf of the GEV distribution evaluated at the perception threshold, and corresponds to the contribution of a censored data (i.e. below the threshold) to the likelihood. The term $p(\tilde{X}_t^{(k)} | \mu, \lambda, \xi, \gamma_k)$ corresponds to the contribution of an observation to the likelihood. It is evaluated with equation (9) or (10) for interval or point data, respectively.

Assuming prior independence, the posterior pdf can then be derived (up to a constant of proportionality) as follows:

$$\begin{aligned} p(\mu, \lambda, \xi, \gamma | \mathbf{X}) &\propto p(\mathbf{X} | \mu, \lambda, \xi, \gamma) p(\mu, \lambda, \xi, \gamma) \\ &\propto p(\mathbf{X} | \mu, \lambda, \xi, \gamma) p(\mu) p(\lambda) p(\xi) \prod_{k=1, Nc} p(\gamma_k) \end{aligned} \quad (12)$$

In this case study, the joint prior distribution of the three GEV parameters is obtained by assuming their prior independence and by using very broad, uniform distributions for location (μ) and scale (λ) parameters. For the shape parameter ξ , we use a Gaussian distribution centred on zero with a standard deviation of 0.3, which means that the interval $[-0.6 ; 0.6]$

contains over 90% of the prior density. Such a prior distribution for the shape parameter is similar to the “geophysical prior” of Martins and Stedinger (2000). Thus:

$$p(\mu, \lambda, \xi) = U(\mu | -10000, 10000) U(\lambda | 0, 10000) N(\xi | 0, 0.3^2) \quad (13)$$

The assumption of prior independence is mainly used here for convenience. However, since flat priors are used for the location and scale parameters in order to reflect the lack of prior knowledge on these parameters, it seems natural not to introduce any form of dependence between them. Importantly, prior independence does not imply that the parameter posterior distributions will be independent (i.e., the parameter estimates might be dependent). Moreover, methods for specifying an informative prior distribution (without necessarily using the assumption of prior independence) have been proposed (e.g. Coles and Powell, 1996; Renard et al., 2006a; Ribatet et al., 2006) and could be used within this inference framework.

The prior distributions of rating curve error parameters γ remains to be specified. This can be done using the results of the hydraulic sensitivity study (Figure 5). More accurately, a triangular prior distribution is used (Figure 6). The mode of this distribution is obtained for $\gamma=1$ (no error), while the base expands between values *min* and *max*. These values are determined so that the corresponding rating curves (thick lines in figure 4) roughly match the limits given by the hydraulic sensitivity analysis. In this case study, these values [*min*; *max*] are equal to [0.8; 1.3] for the historical rating curve and [0.8; 1.25] for the recent rating curve. Note that the choice of such a triangular distribution is somewhat arbitrary. Alternative assumptions may be used (e.g. O'Connell, 2005; O'Connell, et al., 2002). However, this choice is a delicate issue, since a hydraulic sensitivity analysis does not provide the full distribution of the rating curve error. This would require a more in-depth probabilistic assessment of the propagation of errors in the hydraulic model. This is considered to lie beyond the scope of this paper and is left for future work.

Lastly, Markov chain Monte Carlo (MCMC) algorithms are applied to the posterior distribution (12), making it possible to estimate the parameters and derived quantities, including flood quantiles. We used the two-stage MCMC strategy proposed by Renard *et al.* (2006b) . We refer to this paper for a detailed description of the algorithms used. Shortly, the first stage of the algorithm is an adaptive Gibbs sampler (Geman and Geman, 1984), which is used to perform a preliminary exploration of the posterior distribution properties (notably in terms of posterior covariance). In a second step, a standard Metropolis sampler (Metropolis and Ulam, 1949; Metropolis et al., 1953) is used, with a Gaussian jump distribution whose covariance matrix is specified using the preliminary exploration performed at stage one. The Metropolis sampler is ran during 100,000 iterations, with the first half of the iterations being considered as a burn-in period and being therefore discarded. Convergence was assessed by evolving four parallel chains and verifying that the Gelman-Rubin criteria (Gelman et al., 1995) were close to one for all inferred quantities.

3. Results

The modelled series (Figure 2) stems from two information sources: i) data from the flood warning gauge at Anduze (1892-2005), and ii) data from the historical survey, covering the 1741-1891 period. The systematic period is exceptionally long at this site, lasting over 100 years. Over the historical period, the perception threshold was taken to be 2961 m³/s, corresponding to the station's alert level. It should be remembered that discharge values are reconstructed on the basis of one recent (post-1985) and one historical (pre-1985) rating curve.

In a first step, the posterior distribution of GEV parameters obtained with the whole dataset (1741-2005) is evaluated. Figure 7 compares the posterior pdfs obtained when systematic/independent errors are accounted for (thick black lines) or ignored (thin grey lines). It shows that the location and scale parameters estimates are highly sensitive to the treatment of errors affecting data. Conversely, the shape parameter remains similar: this can be explained by the fact that the shape parameters of observed and true runoffs are identical (see appendix 1) with the error model (7) assumed in this study. The posterior pdfs of the multiplicative error terms γ_1 and γ_2 contain the value 1: the probabilistic model identifies no systematic rating curve error.

In a second step, the impact of additional historical information is evaluated by comparing quantiles obtained using the 1892-2005 data with quantiles obtained using the whole 1741-2005 dataset (Figure 8). Note that the treatment of systematic/independent errors is identical in both cases, with all errors being accounted for. Using historical data (pre-1892) appreciably changes the estimated quantiles, owing to the presence of many events in the vicinity of 4000 m³/s. The fit with empirical frequencies is not very satisfactory, but given the shape suggested by these empirical frequencies, it seems likely that no curve would fit these points convincingly.

4. Sensitivity analysis

Section 3 illustrated the impact of errors affecting discharge estimates when historical information is included in the inference. In this analysis, several quantities are fixed prior to the inference: (i) the width of the triangular prior (Figure 6) for systematic rating curve errors; (ii) the width of the discharge uncertainty intervals due to independent errors affecting water levels (intervals in figure 2); (iii) the value of the perception threshold. A sensitivity analysis

is carried out in this section to evaluate whether modifications of these predefined quantities significantly impact the estimated quantiles.

Sensitivity to the triangular prior for rating curve errors is studied by increasing/decreasing the width of the triangle base. More precisely, the original triangle with base $[a;b]$ is replaced by a triangle with base $[a';b']$ defined by:

$$\begin{aligned} a' &= a - z(1 - a) \\ b' &= b + z(b - 1) \end{aligned} \quad (14)$$

z corresponds to an inflation factor. When $z = 0$, the interval $[a;b]$ is unchanged; when $z = 1$, the width of the interval is doubled; when $z = -1$, the interval collapses to the single point 1. The latter case yields a Dirac prior distribution, which corresponds to ignoring the rating curve systematic error.

Sensitivity to the intervals describing independent discharge errors (ε_i , equation (6)) makes use of a similar inflation factor, except that the value 1 in equation (14) is replaced by the centre of the interval $[a;b]$:

$$\begin{aligned} a' &= a - z((a + b) / 2 - a) \\ b' &= b + z(b - (a + b) / 2) \end{aligned} \quad (15)$$

Lastly, the sensitivity to the choice of the perception threshold u is studied by increasing/decreasing the value of u . When u is decreased, the historical information is preserved but its exhaustiveness occurs for a lower discharge. In some sense, decreasing the perception threshold therefore tests the robustness of the inference when the exhaustiveness

assessment is unduly optimistic. Conversely, when u is increased, all historical floods becoming smaller than u are discarded from the analysis.

Results from the sensitivity analysis are shown in figure 9 and yield interesting observations:

- (i) The prior for rating curve systematic errors exerts a significant influence on the estimated quantiles. In particular, the uncertainty strongly increases with the prior width. This demonstrates the influence of the chosen prior distributions on the estimates, and calls for further research to derive meaningful priors from the hydraulic analysis.
- (ii) Independent discharge errors stemming from imprecise knowledge of the water levels appear to impact the results to a lesser extent. In particular, ignoring these errors ($z = -1$) leaves the original estimated quantiles ($z = 0$) almost unchanged.
- (iii) The choice of the perception threshold also exerts a significant influence on the inference, with the estimated quantiles being impacted by both increases and decreases of the threshold. As expected, the inference using historical information becomes similar to the inference solely using the data from the recent period when the threshold reaches high levels ($u = 5,000$ or $10,000 \text{ m}^3 \cdot \text{s}^{-1}$).

Although interesting, these observations should not be extrapolated beyond this particular case study. In particular, the relative influence of systematic and independent errors might be case-specific. This will be established in future work.

IV DISCUSSION

The approach detailed for the Anduze catchment was also applied to the other four catchments of the Gard river listed in section 2. For all of these catchments, the following conclusions may be drawn. First, the use of historical data shows that Frechet-type distributions seem to represent flood discharge distributions better than the Gumbel distribution. For these catchments, the posterior distributions of the shape coefficient indicate that the coefficients are significantly different from zero, ranging from -0.25 at Alès to -0.5 at Anduze. The high values of the shape coefficient for the two main tributaries of the Gardon d'Anduze (Mialet and St-Jean) are consistent with the estimates at Anduze. We reach here the same conclusions as those obtained by Naulet *et al.* (2005) for the Ardèche river and Payrastre *et al.* (2005) for four catchments of the Aude river system. Thus, even when the systematic period is exceptionally long – over 100 years – the distributions of discharge values are clearly modified when historical floods are taken into account. Table 1 presents the estimates of the 10-year and 100-year quantiles for the four catchments with their respective confidence intervals. It can be seen that the ratio of the 100-year quantiles for the historical period to those for the systematic period ranges from 1.1 for the Gardon de Mialet to 1.85 for the Gardon d'Anduze at Anduze. This indicates once again the importance of taking historical flood data into consideration in the predetermination of flood volumes, even when long systematic time series are available.

Examination of the confidence intervals of the quantiles shows that, in contrast to what one might expect, these intervals can become wider when historical floods are taken into account compared to the systematic period alone. This result may be due to the high level of uncertainty affecting the highest historical floods and to the model used for systematic errors.

The specific 100-year flood discharge values obtained when the historical period is used range from 5 to 10 m³/s/km², a standard order of magnitude for Mediterranean catchments. More specifically, we tried to compare our estimates of 100-year flood discharge (Q₁₀₀) with other approaches (Table 2). The empirical relationships established for the Gard region by Bressand and Golossov (1996) give:

$$Q_{\text{rare}} = 30 A^{0.75} \quad \text{and} \quad Q_{\text{exc.}} = 50 A^{0.75} \quad (13)$$

where Q_{rare} and $Q_{\text{exc.}}$ give orders of magnitude for 100-year and 1000-year flood discharge respectively, for a catchment with a surface area A .

Our estimates of Q₁₀₀ using the historical data lie in an interval of -30% to +50% with respect to Q_{rare} . The historical 100-year flood discharge is higher than these estimates for the Anduze and Saint-Jean du Gard catchments. In addition, except in the case of the Gardon d'Anduze, these specific 100-year discharge values are below the highest regional curves of specific discharge values Q_{max} from major floods in Europe, constructed by Stanescu (2004) from a database of more than 700 flood events.

The specific discharge estimate of Q₁₀₀ issued from a regional stochastic rainfall generator mixed with a rainfall-runoff model (Arnaud *et al.*, 2007), called Shyreg model, presents less variations among the four catchments. It seems more logical as the four basins have similar climatic and morphometric characteristics. Q₁₀₀ estimates at Ales and Mialet are similar, as large differences between historical and Shyreg approaches are observed at St Jean (9,6 versus 6,4) and especially at Anduze (9,5 versus 3,8). Large uncertainties on discharge estimates could explain such differences. Additional studies, based on both historical and

regional approaches, are needed to better understand the advantages and limits of each kind of information.

V CONCLUSIONS

A three-step procedure has been used to estimate discharge from major floods on the various Gardon catchments.

First, a historical survey identified and collected data on historical floods. The recent period is particularly rich in information on the studied catchments: the archives of daily discharge readings preserved by the flood forecasting department (FFD) allowed us to reconstruct the time series back to 1892, when the FFD was created. Information in the archives of the Gard region allowed us to supplement the Anduze time series with 29 unindexed flood events that occurred between 1741 and 1891. In view of this research, we can guarantee that the sample is complete for all floods since 1741 that exceeded the 1892 alert level.

These data were then used to reconstruct flood discharge series and their uncertainty, based on a hydraulic model. Several models were constructed for each site in order to take account, to the extent possible, of geomorphological changes in the riverbeds and changes in flood gauges during the period analysed. Recent and historical rating curves were constructed. For a given water level reading, they output a central discharge value with an uncertainty interval that takes account of the roughness of the channel in the reach considered. When this is cumulated with the uncertainty affecting water level readings, the overall uncertainty for the largest floods can be very high, with the relative error of the reconstructed discharge values reaching 100% in some cases.

556

557 Lastly, a Bayesian frequency analysis is performed in order to analyze the sample of recent
558 and historical maxima, accounting for additive and multiplicative error affecting discharge
559 values, respectively due to random error in water level readings and systematic rating curve
560 error.

561

562 The use of historical flood data yielded mixed results. It lengthens the study period, but the
563 reconstructed discharge values are in some cases subject to very high uncertainty, which is
564 due among other things to the rating curves and affects recent discharge values as well. This
565 demonstrates the need to improve discharge measurement, notably by increasing the number
566 of flood gauges, so as to reduce the sources of uncertainty, at least for recent discharge values.
567 When this uncertainty affecting discharge is taken into account in the probabilistic model, the
568 confidence intervals for quantiles are in some cases higher when historical flood data are used
569 than when the analysis is based solely on the recent discharge series. This demonstrates the
570 need for careful evaluation of the various sources of uncertainty in order to assess the impact
571 of using historical flood data and for their integration in the probabilistic model. In addition,
572 the historical quantiles have been found of the same order of magnitude as those obtained
573 through regional empirical methods, for two of the four studied catchments.

574

575

575 Appendix 1

576 The aim is to derive the distribution of $\tilde{X}_t^{(k)} = X_t / \gamma_k - \varepsilon_t$, conditionally on errors γ_k and ε_t .

577 For this purpose, let us write the cdf of $\tilde{X}_t^{(k)}$ at a given value x :

$$\begin{aligned} \Pr(\tilde{X}_t^{(k)} \leq x) &= \Pr(X_t / \gamma_k - \varepsilon_t \leq x) \\ &= \Pr(X_t \leq \gamma_k(x + \varepsilon_t)) \end{aligned} \quad (16)$$

578 Since $X_t \sim GEV(\mu, \lambda, \xi)$, equation (1) yields:

$$\begin{aligned} \Pr(\tilde{X}_t^{(k)} \leq x) &= \Pr(X_t \leq \gamma_k(x + \varepsilon_t)) \\ &= \exp\left\{-\left[1 - \xi(\gamma_k(x + \varepsilon_t) - \mu) / \lambda\right]^{1/\xi}\right\} \\ &= \exp\left\{-\left[1 - \gamma_k \xi(x + \varepsilon_t - \mu / \gamma_k) / \lambda\right]^{1/\xi}\right\} \\ &= \exp\left\{-\left[1 - \xi(x - (\mu / \gamma_k - \varepsilon_t)) / (\lambda / \gamma_k)\right]^{1/\xi}\right\} \end{aligned} \quad (17)$$

579 The latter expression is equal to the cdf of a $GEV(\mu / \gamma_k - \varepsilon_t, \lambda / \gamma_k, \xi)$ evaluated at x .

580

581 Appendix 2

582 The aim is to perform the following integration:

$$p(\tilde{X}_t^{(k)} | \mu, \lambda, \xi, \gamma_k) = \int p(\tilde{X}_t^{(k)} | \mu, \lambda, \xi, \gamma_k, \varepsilon_t) p(\varepsilon_t) d\varepsilon_t \quad (18)$$

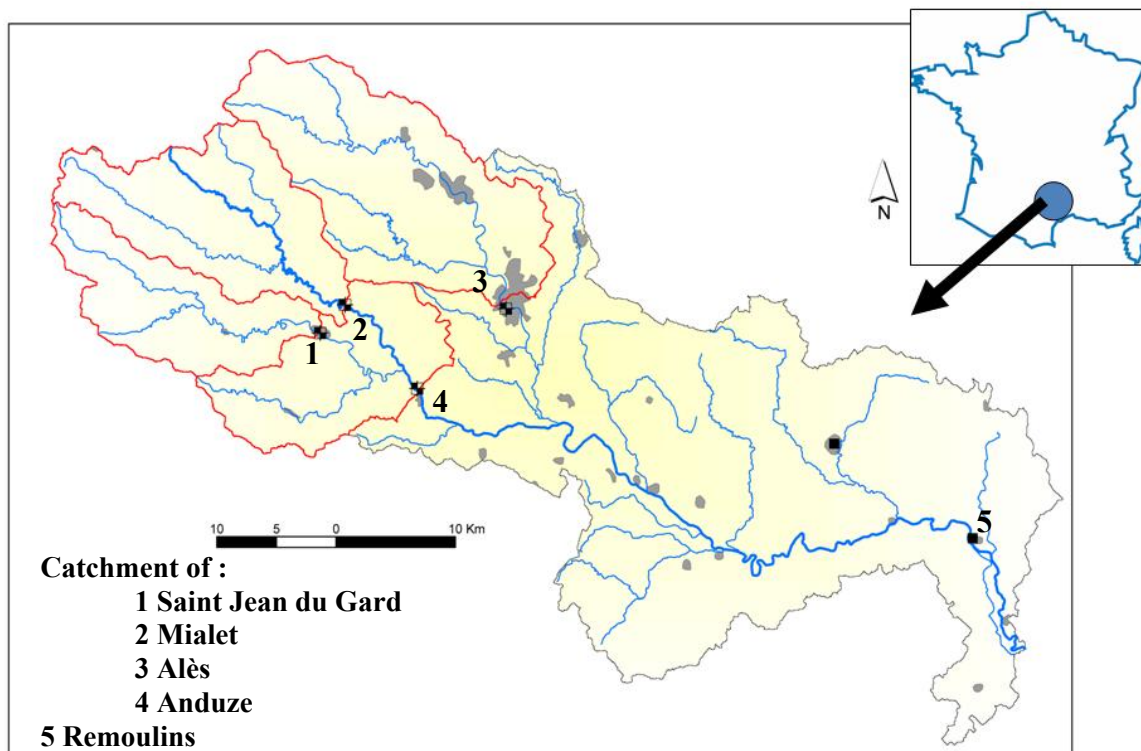
583 Assuming $p(\varepsilon_t)$ is a uniform distribution on $[a_t, b_t]$ yields:

$$\begin{aligned} p(\tilde{X}_t^{(k)} | \mu, \lambda, \xi, \gamma_k) &= \int_{a_t}^{b_t} f(\tilde{X}_t^{(k)} | \mu / \gamma_k - \varepsilon_t, \lambda / \gamma_k, \xi) \frac{1}{b_t - a_t} d\varepsilon_t \\ &= \frac{1}{b_t - a_t} \int_{a_t}^{b_t} (\gamma_k / \lambda) \left[1 - \xi \gamma_k (\tilde{X}_t^{(k)} - \mu / \gamma_k + \varepsilon_t) / \lambda\right]^{\frac{1}{\xi}-1} \exp\left\{-\left[1 - \xi \gamma_k (\tilde{X}_t^{(k)} - \mu / \gamma_k + \varepsilon_t) / \lambda\right]^{1/\xi}\right\} d\varepsilon_t \end{aligned} \quad (19)$$

584 Using the substitution $u = \tilde{X}_t^{(k)} + \varepsilon_t$:

$$\begin{aligned}
& p(\tilde{X}_t^{(k)} \mid \mu, \lambda, \xi, \gamma_k) \\
&= \frac{1}{b_t - a_t} \int_{\tilde{x}_t^{(k)} + a_t}^{\tilde{x}_t^{(k)} + b_t} (\gamma_k / \lambda) [1 - \xi \gamma_k (u - \mu / \gamma_k) / \lambda]^{\frac{1}{\xi} - 1} \exp \left\{ - [1 - \xi \gamma_k (u - \mu / \gamma_k) / \lambda]^{1/\xi} \right\} du \\
&= \frac{1}{b_t - a_t} \int_{\tilde{x}_t^{(k)} + a_t}^{\tilde{x}_t^{(k)} + b_t} f(u \mid \mu / \gamma_k, \lambda / \gamma_k, \xi) du \\
&= \frac{1}{b_t - a_t} \left[F(\tilde{x}_t^{(k)} + b_t \mid \mu / \gamma_k, \lambda / \gamma_k, \xi) - F(\tilde{x}_t^{(k)} + a_t \mid \mu / \gamma_k, \lambda / \gamma_k, \xi) \right]
\end{aligned} \tag{20}$$

585



586

587 **Figure 1: Overview of the four studied catchments**

588

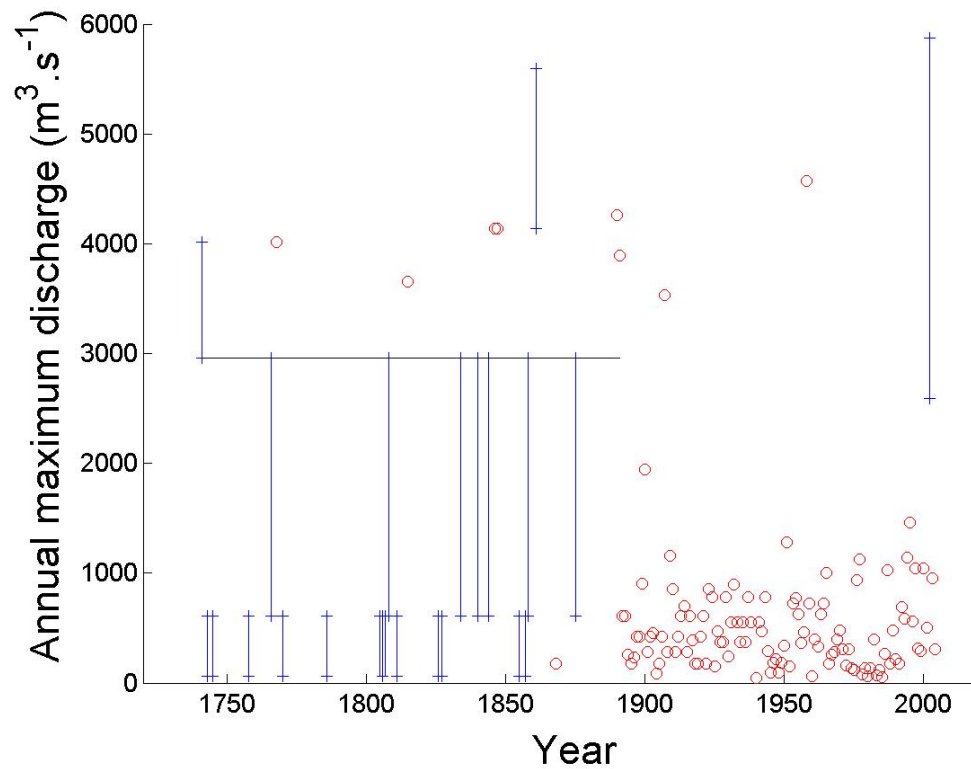


Figure 2: Floods on the Gardon d'Anduze river at Anduze (1741-2005). Circles correspond to events whose water level is known with high precision. Intervals represent the uncertainty due to imperfect knowledge of the water level reached during the event. The horizontal line is the perception threshold.

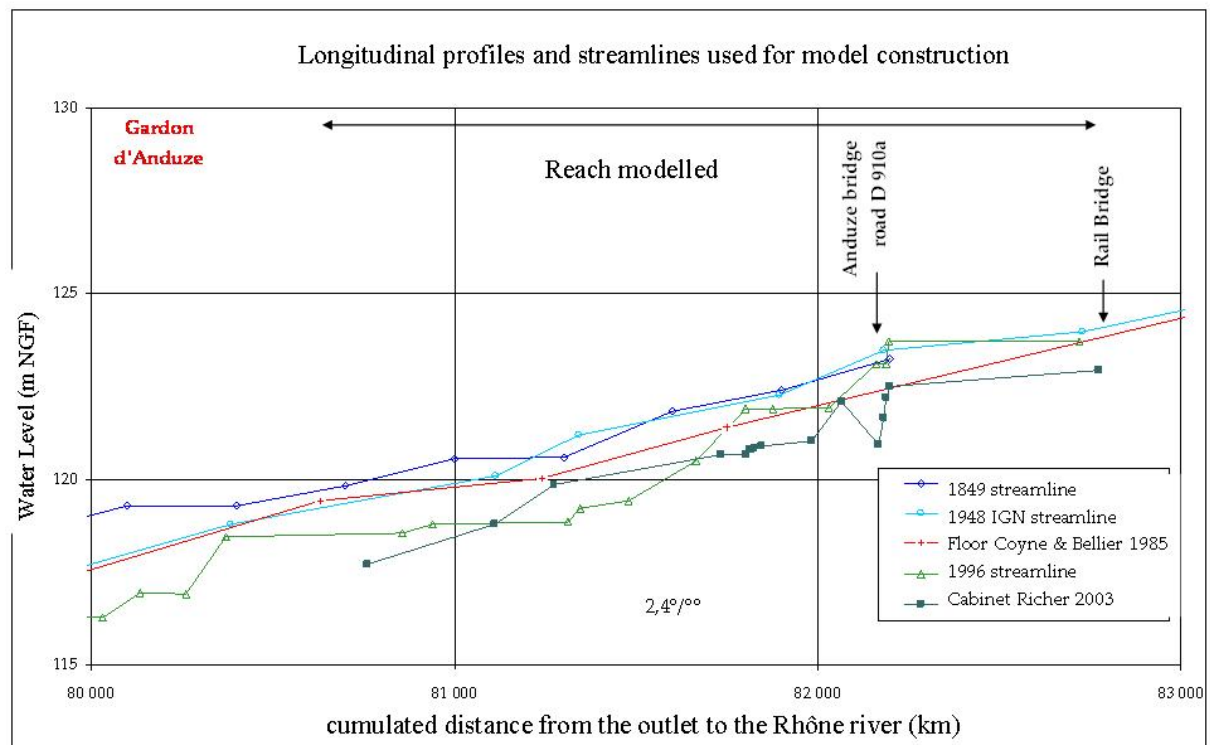


Figure 3: Longitudinal profile of the Gardon d'Anduze river at Anduze

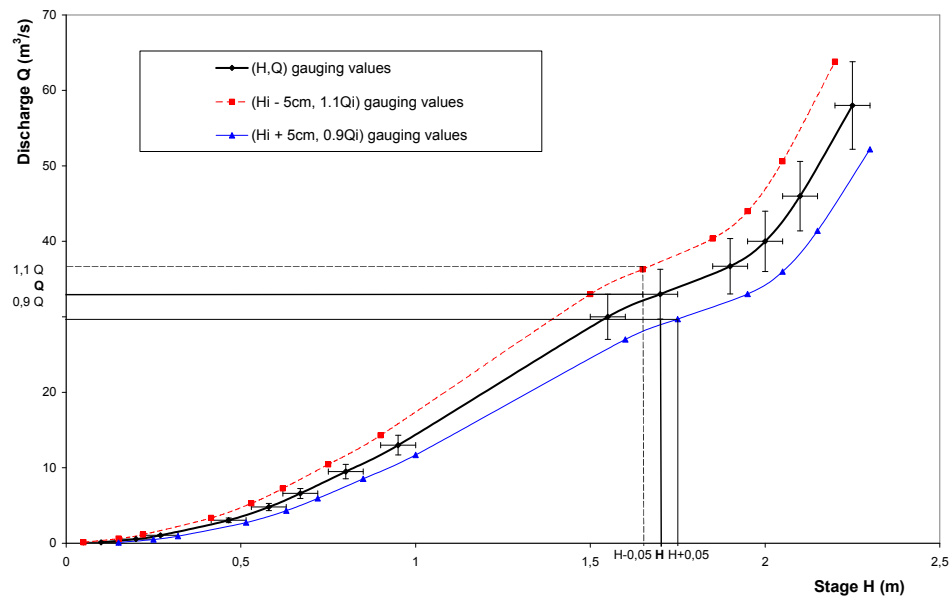


Figure 4: Envelope curves of the stage-discharge relationship

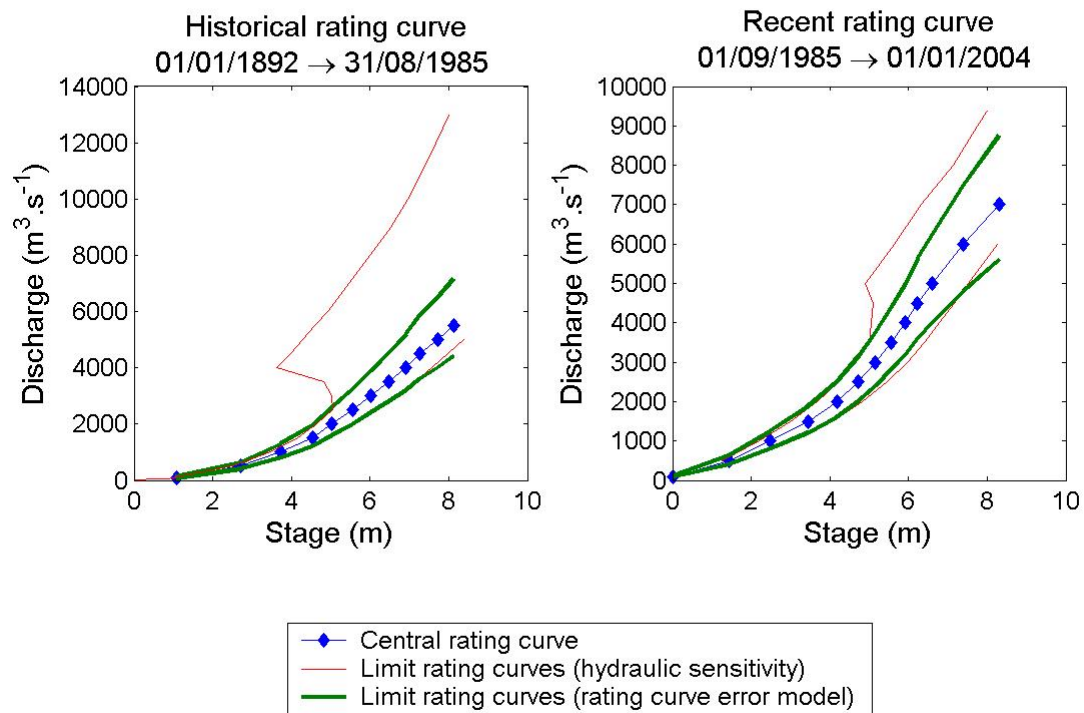


Figure 5: Historical and recent rating curves

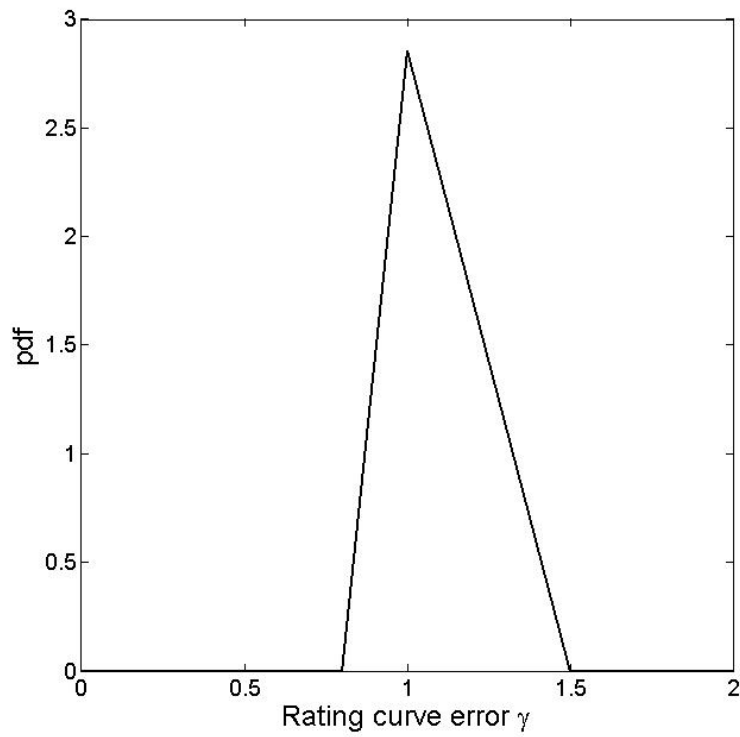


Figure 6: Illustration of a triangular prior pdf for the rating curve error parameter γ

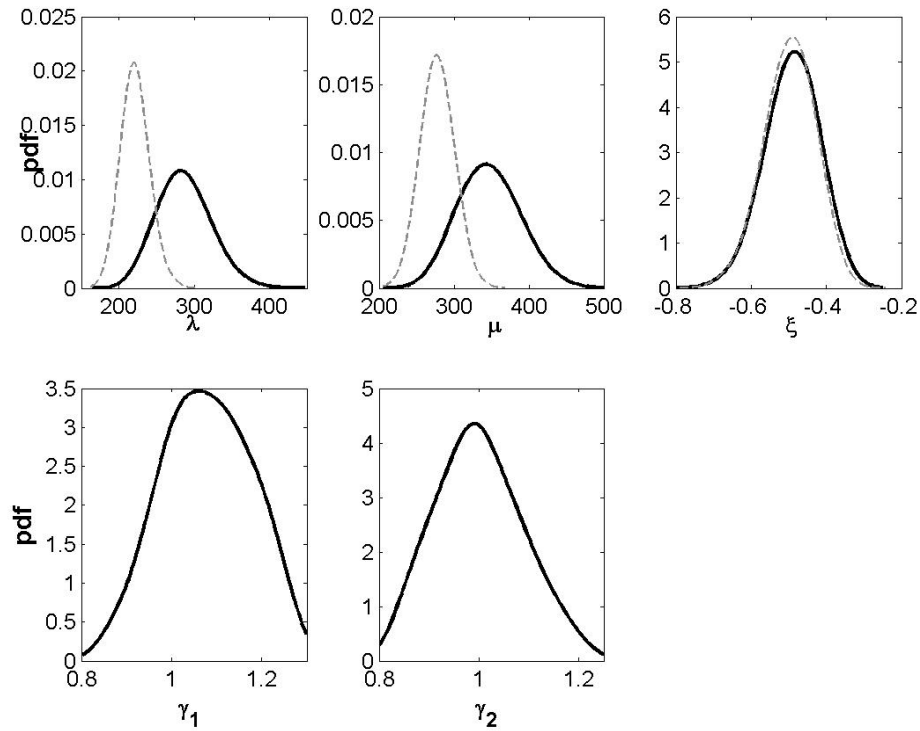


Figure 7: Posterior pdfs of GEV parameters λ , μ , ξ , and of rating curve error parameters γ_1 and γ_2 , obtained with the whole dataset 1741-2005. Thick black lines = systematic and independent errors accounted for; thin grey lines: systematic and independent errors ignored.

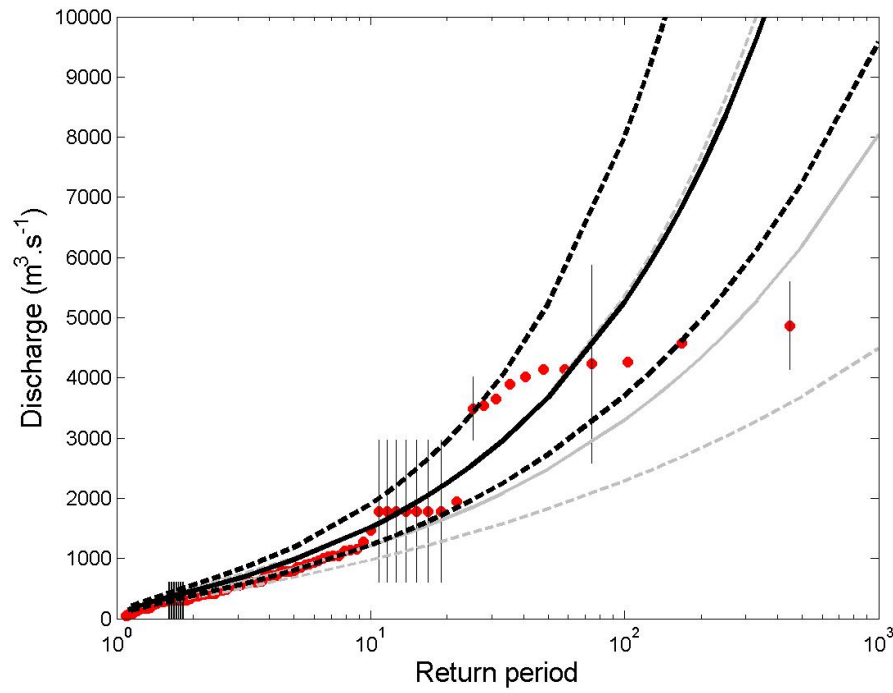


Figure 8: GEV distribution of annual maxima at Anduze, with 90% posterior intervals

Note: Thick lines = whole period (1741-2005); thin lines = the systematic period (1892-2005); circles = empirical frequencies.

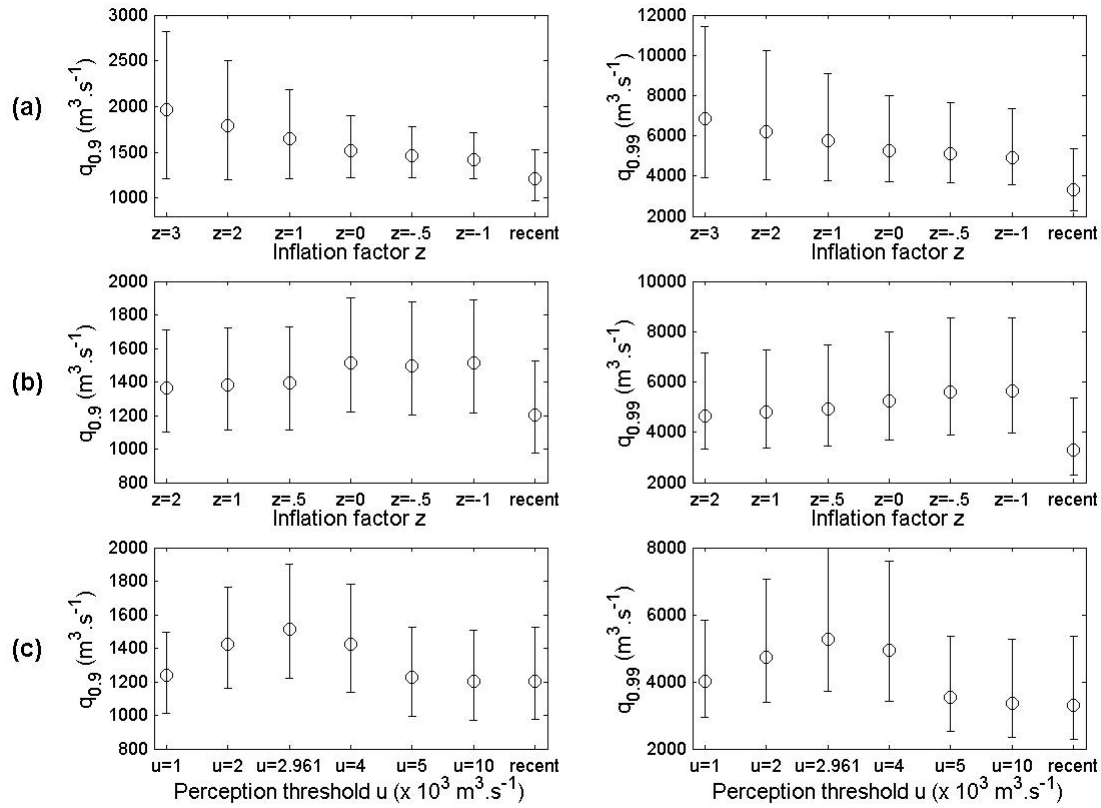


Figure 9: Sensitivity of 0.9- and 0.99-quantiles posterior estimates. Circles represent posterior medians, bars represent 90% posterior intervals. (a) Sensitivity to the prior for systematic rating curve errors; (b) sensitivity to the width of intervals describing independent errors; (c) sensitivity to the perception threshold. ‘recent’ denotes results with data from the period 1892-2005 (with rating curve errors accounted for).

	Systematic period		Historical period	
Catchment (area)	Q10 +/-IC 90% (m ³ /s)	Q100 +/- IC 90% (m ³ /s)	Q10 +/- IC90% (m ³ /s)	Q100 +/- IC90% (m ³ /s)
Anduze (540 km ²)	1070 +240/-170	2780 +1680/-800	1460 +360/-290	5130 +2650/-1540
Alès (320 km ²)	690 +370/-80	1330 +550/-530	770 +130/-120	1650 +480/-340
Mialet (219 km ²)	250 +90/-60	1170 +1110/-460	270 +80/-60	1250 +770/-420
Saint-Jean (154 km ²)	300 +80/-60	920 +680/-300	360 +100/-70	1480 +900/-480

Table 1: 10-year and 100-year quantiles in m³/s estimated on the basis of the systematic and historical periods, and their 90% confidence intervals

]

Catchments (area)	Q100 with historical data	Q _{rare} Q _{exc.} (Bressand and Golossof, 1996)	Q _{max} (Stanescu, 2004)	Shyreg (Arnaud and Lavabre, 2007)
Anduze (540 km ²)	9.5	6.2 10.4	7.8	3.8
Alès (320 km ²)	5.2	7.1 11.8	10	5.1
Mialet (219 km ²)	5.7	7.8 13.0	12.8	5.4
Saint- Jean (154 km ²)	9.6	8.5 14.2	13.9	6.4

Table 2: Comparison of specific discharge estimates (m³/s.km²) for 100-year quantiles or major floods on the Gardon rivers

Bibliographical references

- Arnaud P., Lavabre J., Sol B., Desouches C., 2007. Régionalisation d'un générateur de pluies horaires sur la France métropolitaine pour la connaissance de l'aléa pluviographique. *Hydrological Sciences Journal*, 53 (1), 34-47.
- Ayral P.A., 2005. Contribution à la spatialisation du modèle opérationnel de prevision des crues éclair ALTHAIR, approches spatiale et expérimentale ; application au bassin versant du Gardon d'Anduze. MSc Thesis, University d'Aix Marseille, 311 p.
- Barnes H.H., 1967. Roughness Characteristics of Natural Channels. U.S. Geological Survey, Water Supply Paper 1849.
<http://wwwrcamnl.wr.usgs.gov/sws/fieldmethods/Indirects/nvalues/index.htm>
- Brazdil R., Kundzewicz Z.W., Benito G., 2006. Historical hydrology for studying flood risk in Europe. *Hydrological Sciences Journal*, 51 (5), 739-764.
- Bressand F., Golossof G., 1996. Méthode de calcul des débits rares et exceptionnels d'eaux pluviales sur les petits bassins versants naturels situés dans l'arc méditerranéen. DDE (Infrastructure Department) for the Gard region (France), Water and Environment unit, 42 pp.
- Chow, V.T., 1960. Open Channel hydraulics, Mc Graw Hill Book Company, New-York, 380p.

- 672 Cœur D., Lang M., Paquier A., 2002. L'historien, l'hydraulicien et l'hydrologue et la
673 connaissance des inondations. *La Houille Blanche*, 4/5, 61-66.
674
- 675 Coles, S. G., and E. A. Powell, 1996. Bayesian methods in extreme value modelling: A
676 review and new developments, *Int. Stat. Rev.*, 64, 119-136.
677
- 678 DDE (*Direction Départementale de l'Équipement* – Infrastructure Department) of the Gard
679 region (France), 2003. Validation des relevés hydrométriques de la crue du 08 et 09
680 septembre 2002. SOGREAH internal report, no. 102793, November 2003, 98 pp.
681
- 682 Delrieu G., Kirstetter P-E., Nicol J., Neppel L., 2004. L'événement pluvieux des 08 et 09
683 septembre 2002 dans le Gard : estimation des précipitations par radars et pluviomètres. *La*
684 *Houille Blanche*, 6, 93-98.
685
- 686 Embrecht C., Kluppelberg C., Mikosch T., 1997. *Modelling Extremal Events for Insurance*
687 *and Finance*. Springer-Verlag, Berlin.
688
- 689 Gaume E., Livet M., Desbordes M., Villeneuve J.P., 2004. Hydrological analysis of the river
690 Aude, France, flash flood on 12 and 13 November 1999. *Journal of Hydrology*, 286, 135-154.
691
- 692 Gelman, A., et al., 1995. *Bayesian data analysis*, 526 pp., Chapman & Hall.
693
- 694 Gob F., Jacob N., Bravard J.P., Petit F., 2008. The value of lichenometry and historical
695 archives in assessing the incision of submediterranean rivers from the Little Ice Age in the
696 Ardèche and upper Loire (France). *Geomorphology*, 94, 170-183.

697

698 Hirsh R.M., Stedinger J.R., 1987. Plotting positions for historical floods and their precision.
699 *Water Resources Research*, 22(4), 715-727.

700

701 Huet P., Martin X., Prime J.L., Foin P., Laurain C., Cannard P., 2003. Retour d'expérience
702 des crues de septembre 2002 dans les départements du Gard, de l'Hérault, du Vaucluse, des
703 Bouches du Rhône, de l'Ardèche et de la Drôme. Report of the General Inspectorate for the
704 Environment, Ministry of Ecology, Energy, Sustainable Development and Regional Planning
705 (MEEDDAT), 133 pp.

706 <http://www.ecologie.gouv.fr/-Rapports-de-l-Inspection-generale-.html>.

707

708 ISL Bureau d'Ingenieurs Conseils, 2005. Référentiel hydrologique sur le bassin versant des
709 Gardons. DDE (Infrastructure Department) of the Gard region, internal report.

710

711 Jacquet J., 1959. Les crues d'automne 1958 sur le Vidourle. *Mémoire et travaux de la société*
712 *hydrotechnique de France*, (1)11: 66-82.

713

714 Kuczera, G., 1992. Uncorrelated measurement error in flood frequency inference, *Water*
715 *Resources Research*, 28, 183-188.

716

717 Kuczera, G., 1996. Correlated rating curve error in flood frequency inference, *Water*
718 *Resources Research*, 32, 2119-2127.

719

720 Lang M., Perret C., Renouf E., Sauquet E., Paquier A., 2006. Incertitudes sur les débits de
721 crue. *La Houille Blanche*, 6, 33-41

722

723 Llasat C., Barriendos M., Barrera A., Rigo T., 2005. Floods in Catalonia (NE Spain) since the
724 14th century. Climatological and meteorological aspects from historical documentary sources
725 and old instrumental records. *Journal of Hydrology*, 313, 32-47.

726

727 Martins, E. S., and J. R. Stedinger, 2000. Generalized maximum-likelihood generalized
728 extreme-value quantile estimators for hydrologic data, *Water Resources Research*, 36, 737-
729 744.

730

731 Naulet R., 2002. Utilisation de l'information des crues historiques pour une meilleure
732 prédétermination du risque d'inondation. Application au bassin de l'Ardèche à Vallon Pont
733 d'Arc et à St Martin d'Ardèche. PhD diss., Université Joseph Fourier Grenoble, Université du
734 Québec INRS, Cemagref Lyon, 322 pp.

735

736 Naulet R., Lang M., Ouarda Taha B.M.J., Coeur D., 2005. Flood frequency analysis on the
737 Ardèche river using French documentary sources from the last two centuries. *Journal of*
738 *Hydrology*, 313, 58-78.

739

740 Neppel L., Bouvier C., Vinet F., Desbordes M., 2003. Sur l'origine de l'augmentation des
741 inondations en région méditerranéenne. *Revue des Sciences de l'Eau*, 16 (4), 475-494.

742

743 Neppel L. *et al.*, 2007. InondHis-LR : analyse des précipitations et crues anciennes en région
744 Languedoc-Roussillon. RDT programme, Ministry of Ecology, Energy, Sustainable
745 Development and Regional Planning (MEEDDAT), contract CV04000067, 209 pp.

746

Marchandise A., 2007. Modélisation hydrologique distribuée sur le Gardon d'Anduze ; étude comparative de différents modèles pluie-débit, extrapolation de la normale à l'extrême et tests d'hypothèses sur les processus hydrologiques, MSc Thesis. University Montpellier II, Montpellier, France.

O'Connel, D. R. H., 2005. Nonparametric Bayesian flood frequency estimation, *J. Hydrol.*, 313, 79-96.

O'Connel, D. R. H., Ostenaar D.A., Levish R., Klinger R.E., 2002. Bayesian flood frequency analysis with paleohydrologic bound data, *Water Resources Research*, 38.

Paquier A., Khodashenas S.R., 2002. River bed deformation calculated from boundary shear stress. *Journal of Hydraulic Research*, 40 (5), 603-609.

Parent, E., and J. Bernier, 2003. Bayesian POT modeling for historical data, *J. Hydrol.*, 274, 95-108.

Payrastre O., Gaume E., Andrieu H., 2005. Use of historical data to assess the occurrence of floods in small watersheds in the French Mediterranean Area. *Advances in Geosciences*, 2, 313-320.

Payrastre O., Gaume E., Andrieu H., 2006. Apport du recueil de données historiques pour l'étude des crues extrêmes de petits cours d'eau ; Etude du cas de quatre bassins versants affluents de l'Aude. *La Houille Blanche*, 6, 79-86.

- Reis, D. S., and J. R. Stedinger, 2005. Bayesian MCMC flood frequency analysis with historical information, *J. Hydrol.*, 313, 97-116.
- Reitan, T., and A. Petersen-Overleir, 2009. Bayesian methods for estimating multi-segment discharge rating curves, *Stochastic Environmental Research and Risk Assessment*. 23(5), 627-642
- Renard B., 2006. Détection et prise en compte d'éventuels impacts du changement climatique sur les extrêmes hydrologiques en France. PhD diss., INP Grenoble, Cemagref Lyon, 361 pp.
- Renard, B., M. Lang, and P. Bois, 2006a. Statistical analysis of extreme events in a non-stationary context via a Bayesian framework., *Stoch. Environ. Res. Risk Assess.*, 21, 97-112.
- Renard B., Garreta V., Lang M., 2006b. An application of Bayesian analysis and MCMC methods to the estimation of a regional trend in annual maxima. *Water Resources Research*, 42.
- Renouf E., Lang M., Sauquet E., Paquier A., 2005. Contrôle de la qualité des courbes de tarage de la banque HYDRO pour les débits de crue. Cemagref report for the Ministry of Ecology and Sustainable Development (MEDD), 53 pp. + annexes (112 pp.).
- Ribatet, M., E. Sauquet, J. M. Gresillon, and T. B. M. J. Ouarda, 2006. A regional Bayesian POT model for flood frequency analysis, *Stoch. Environ. Res. Risk Assess.*, 21, 327-339.

- 796 Sheffer N.A., Rico M., Enzel Y., Benito G., Grodrek T., 2008. The paleoflood record of the
797 Gardon River, France: A comparison with the extreme 2002 flood event. *Geomorphology* 98,
798 71-83, doi:10.1016/j.geomorph.2007.02.034.
799
- 800 Stanescu V.A., 2004. Le potentiel des grandes crues de l'Europe, leur régionalisation et
801 comparaison. *La Houille Blanche*, 6, 21-25.
802
- 803 Thyer, M., B. Renard, D. Kavetski, G. Kuczera, S.W. Franks and S.W. Srikanthan, ?? 2009.
804 Critical evaluation of parameter consistency and predictive uncertainty in hydrological
805 modelling: a case study using bayesian total error analysis, *Water Resources Research*, 45.
806 W00B14
807